Intercalibration of the Infrared Window and Water Vapor Channels on Operational Geostationary Environmental Satellites Using a Single Polar-Orbiting Satellite

MATHEW M. GUNSHOR

Cooperative Institute for Meteorological Satellite Studies, Madison, Wisconsin

TIMOTHY J. SCHMIT

NOAA/NESDIS, Office of Research and Applications, Advanced Satellite Products Team, Madison, Wisconsin

W. PAUL MENZEL

NOAA/NESDIS, Office of Research and Applications, Madison, Wisconsin

(Manuscript received 16 December 2002, in final form 11 June 2003)

ABSTRACT

The Cooperative Institute for Meteorological Satellite Studies (CIMSS) has been intercalibrating radiometers on five geostationary satellites (*GOES-8, -10*, *Meteosat-5, -7,* and *GMS-5*) using a single polar-orbiting or low-earth orbiting satellite [*NOAA-14* High-Resolution Infrared Radiation Sounder (HIRS) and Advanced Very High Resolution Radiometer (AVHRR)] as a reference on a routine basis using temporally and spatially collocated measurements. This is being done for the 11-μm infrared window (IRW) channels as well as the 6.7-μm water vapor (WV) channels. IRW results between AVHRR or HIRS and all five geostationary instruments show relatively small differences, with all geostationary instruments vicariously comparing to within 0.6 K. The WV results between HIRS and all five geostationary instruments show larger differences, with geostationary instruments separating into two groups: *GOES-8, -10,* and *GMS-5* comparing within 1 K; *Meteosat-5* and *-7* comparing within 0.1 K; and the two groups comparing within 2.7 K.

1. Introduction

Satellites traditionally used for daily weather monitoring have proven to be useful in longer-term regional and global environmental monitoring. Thus, the ability to compare the measured radiances from different instruments has become increasingly important. The international meteorological satellite community, represented by the Coordination Group for Meteorological Satellites, has documented a need to validate radiances measured by satellite instruments (Counet 2001). This need is not new, as researchers have compared satellite radiances for earlier instruments such as the Visible Infrared Spin-Scan Radiometer Atmospheric Sounder, *Meteosat-3, -4,* and High-Resolution Infrared Radiation Sounder (HIRS) on *NOAA-11* and *NOAA-12* (Menzel et al. 1981; Schmit and Herman 1992; Desormeaux et al. 1993; Menzel et al. 1993). High-Resolution Interferometer Sounder (HIS) onboard aircraft has been compared to the *GOES-8* Sounder (Menzel et al. 1998). More recently, researchers at the European Organisation for the Exploitation of Meteorological Satellites (EUMETSAT; Tjemkes et al. 2001), the National Aeronautics and Space Administration (NASA; Minnis et al. 2002), and the National Oceanic and Atmospheric Administration (NOAA; Gunshor et al. 2001) have continued with contemporary instruments.

The Cooperative Institute for Meteorological Satellite Studies (CIMSS), located at the University of Wisconsin—Madison, has been intercalibrating radiometers on five geostationary (''geo'') satellites (*GOES-8, -10, Meteosat-5, -7,* and *GMS-5*) using a single polar-orbiting or low-earth orbiting (''leo'') satellite radiometer [*NOAA-14* HIRS and the Advanced Very High Resolution Radiometer (AVHRR)] as a reference on a routine basis using temporally and spatially colocated measurements. This is being done for the 11-μm infrared window (IRW) channels as well as the 6.7-μm water vapor (WV) channels. This paper outlines the method used at CIMSS for satellite intercalibration and summarizes results.

Intercalibration provides valuable information for a wide range of satellite activities. There is an extensive list of quantitative products, many produced operationally, that are made at least in part using either polar or geostationary satellite radiances including sea and land

Corresponding author address: Mathew M. Gunshor, CIMSS, 1225 W. Dayton St., Madison, WI 53706.
E-mail: matg@ssec.wisc.edu

TABLE 1. Satellite instrument details (NASA 1996; EUMETSAT 2000; Suzuki 1997; Kidwell 1998).

Instrument	Launch	Longitude	IRW range (μm)	WV range (μm)	FOV at nadir (km)
GOES-8	1994	75°W	10.2–11.2	6.5–7.0	4 (IRW) or 8 (WV)
GOES-10	1997	135°W	10.2–11.2	6.5–7.0	4 (IRW) or 8 (WV)
Meteosat-5	1991	63°E	10.5–12.5	5.7–7.1	5
Meteosat-7	1997	0°	10.5–12.5	5.7–7.1	5
GMS-5	1995	140°E	10.5–11.5	6.5–7.0	5
NOAA-14 HIRS	1994	LEO	10.9–11.3	6.6–6.9	17.4
NOAA-14 GAC	1994	LEO	10.3–11.3	NA	4

surface temperatures (Wu et al. 1999) and cloud properties (Ellrod 1996). Intercomparison of measured radiances helps to validate the findings of longer-term environmental studies using satellite data. In addition, all numerical forecast models assimilate either satellite radiances or products derived from satellite radiances. Absolute validation is difficult because there currently does not exist a method to measure earth-emitted radiances precisely. Differences between various operational satellite-measured radiances can be determined by continual intercalibration.

Some details for each of the satellite instruments used in this study can be found in Table 1. On Geostationary Operational Environmental Satellites (GOES) the relation between sensor output voltage and radiation energy is treated as nonlinear and a combination of onboard blackbody and space looks are used for onboard calibration (Weinreb et al. 1997). GOES imager data are oversampled in the east–west scan direction by 1.7 km (Menzel and Purdom 1994). On the Geostationary Meteorological Satellite (*GMS-5*) the relation between sensor output voltage and the radiation energy is treated as linear and a combination of onboard blackbody and space looks are used for onboard calibration. *Meteosat-7* has two blackbodies (a cold and a warm reference) and combines these with space looks for onboard calibration. The blackbody system on *Meteosat-7* is used for vicarious calibration of *Meteosat-5* (Tjemkes et al. 2001). The relation between sensor output voltage and radiation energy is treated as linear. *NOAA-14* is a polar-orbiting satellite, hence no reference longitude is included in Table 1. HIRS/2 has two onboard black bodies (warm and cool targets), which are scanned for the entire length of a scan line in addition to a scan line devoted to space look. The relationship between sensor output voltage and radiance is treated as nonlinear. AVHRR/2 uses a blackbody and space looks for onboard calibration and the relationship between sensor output voltage and radiance is treated as linear. There is no water vapor channel on AVHRR.

The various field-of-view (FOV) resolutions, viewing-angle considerations, and time differences between polar-orbiting and geostationary satellites present unique challenges when comparing instruments. In addition, each instrument has a unique spectral response for each channel and not all IRW channels or WV channels cover the same part of the earth-emitted spectrum (Figs. 1 and 2). The following section explains in part how these issues can be managed.

2. Method

The technique for intercalibration has been developed and evolved at CIMSS over the past several years (Wanzong et al. 1998). The original method called for a human operator to search for and collect data, as well as manually run the software to analyze each case. This was time intensive and made collection of large datasets difficult. Implementing computer automation has increased the annual volume of cases collected and analyzed by an order of magnitude. The following paragraphs describe the process of obtaining and processing a single intercomparison case.

There are four automated steps to satellite intercalibration: 1) data collection, 2) data transformations, 3) study area selection, and 4) calculations. The first step, data collection, is the most important. These data, provided by the Space Science and Engineering Center Data Center, are collected in near–real time. It is time consuming to restore data from an archive so processing is best done in near–real time as well.

a. Data collection

Collocation of the polar orbiter and geostationary data in space and time is required. Data are selected within $\pm 10°$ (latitude and longitude) of the geostationary subsatellite point and NOAA radiometer scan angles must be $\pm 14°$ in order to minimize satellite zenith angle differences. These criteria result in a maximum satellite zenith angle of approximately 15° for leo and 16° for geo. Figure 3 illustrates how fast-forward model calculated brightness temperatures for the infrared window and water vapor regions vary by satellite zenith angle from the nadir view (for the standard tropical atmosphere). The difference between a nadir view and the satellite zenith angles for geo and leo will generally be very small (less than 0.1 K) and even at the most extreme angles possible less than approximately 0.3 K in the water vapor channel, where the effect is most pronounced. To maximize scene consistency between the two instruments, geo data are collected within ± 15 min of leo overpass time at the geostationary subsatellite point. For the infrared window channel, the mean ra-

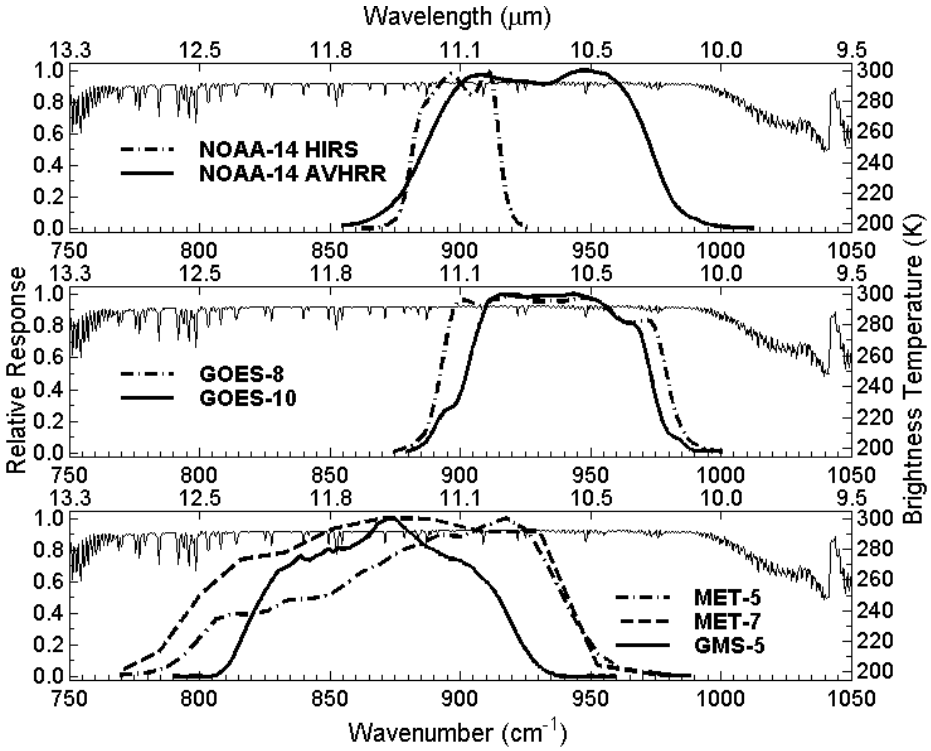

FIG. 1. IRW channel spectral response functions against a sample earth emitted spectrum as measured by aircraft HIS.

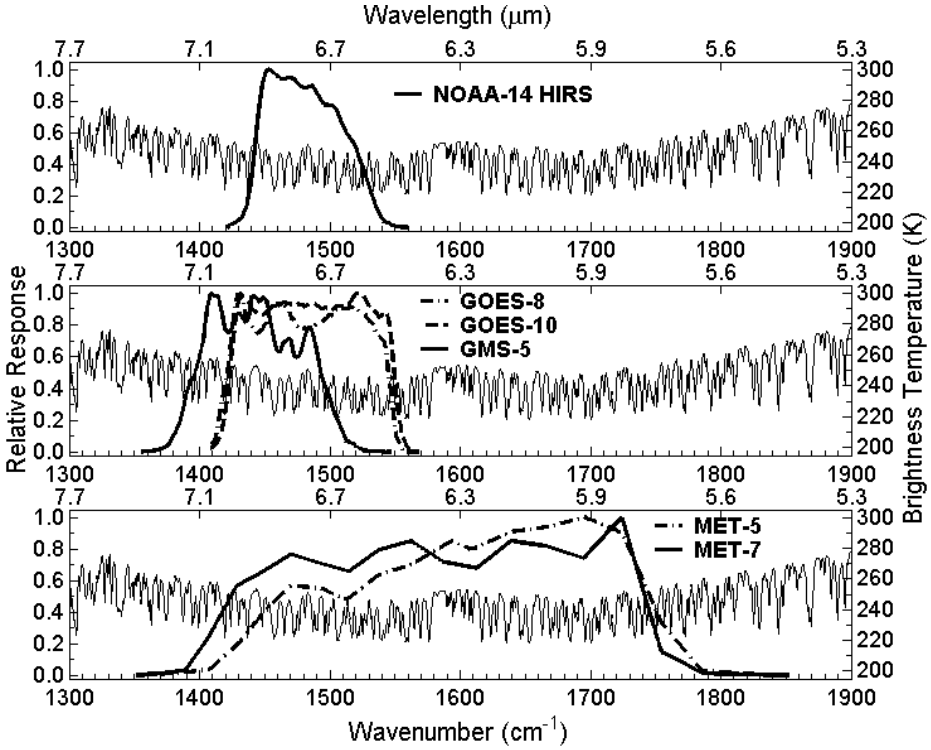

FIG. 2. Water vapor channel spectral response functions against a sample earth-emitted spectrum as measured by aircraft HIS.

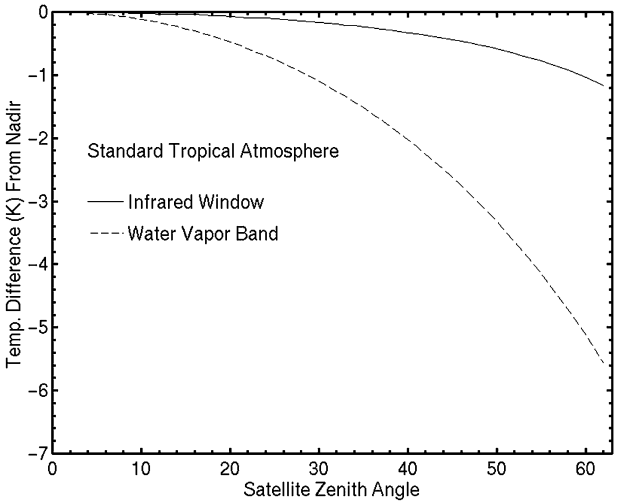

FIG. 3. Fast-forward model calculated brightness temperature variation with satellite zenith angle for the standard tropical atmosphere.

diance in the study area must be greater than 80 mW m^{-2} cm $ster^{-1}$ (or approximately 280 K); there is not a similar test applied to the water vapor channel. This crude test eliminates extremely cloudy scenes; there are no additional attempts made at screening out clouds. Though the CIMSS method of intercalibration does not rely on precise FOV collocation (which will minimize the effects of navigation errors), the introduction of a cold cloud in an otherwise clear scene could skew the results of a comparison if the cloud is at the edge of the scene. For this study, infrared window channel ($\sim$11 μm) and water vapor channel. ($\sim$7 μm) data are collected from each of the operational geostationary instruments (*GOES-10, GOES-8, Meteosat-7, Meteosat-7,* and *GMS-5*) and from HIRS on *NOAA-14.* In addition AVHRR infrared window channel data are collected.

In addition, atmospheric profile data are collected for forward model calculations (section 2d). The equatorial location of the geostationary nadir view data eliminates the use of radiosondes as a consistent (daily) source of this data; atmospheric profiles for these regions from short-term forecasts from global forecast models are used. This study employs the United States Navy Navy Operational Global Atmospheric Prediction System (NOGAPS) model (Rosmond 1992). These data, in their native format, contain 24 vertical levels in a profile, which are converted to 40 levels during the data collection process (as of 18 September 2002 NOGAPS contains 30 levels). The model data are interpolated in space for a given earth location and between forecast hours for a given time.

b. Data transformations

There are a number of data transformations necessary before the comparison can occur. Data, in the form of counts (scaled radiances), from each satellite are smoothed to an effective 100-km resolution to mitigate the effects of different FOV sizes and sampling densities. HIRS undersamples with a 17.4-km nadir FOV, AVHRR Global Area Coverage (GAC) achieves 4 km resolution by resampling, GOES imager oversamples 4 km FOVs in the east–west by 1.7 km, and *Meteosat-5, Meteosat-7,* and *GMS-5* sample a nadir 5-km FOV contiguously. This image smoothing is done using a running average; the resultant image has the same number of pixels as the original; however, each pixel is the average of the approximate 10 000 km^2 surrounding it.

Scaled radiances, commonly referred to as counts, are converted to radiances with a linear conversion; this process is described for the GOES variable format data stream by Weinreb et al. (1997) and a similar process is followed for the other instrument data streams. An additional conversion is necessary for Meteosat instruments since those data are provided in radiance units of W m^{-2} $ster^{-1}$, not the spectral radiance units of mW m^{-2} $ster^{-1}$ cm. This conversion is accomplished by dividing by the integral of the spectral response function. Tests show that some error (less than 0.5 K in the IRW) may be introduced by uncertainty in the spectral response function.

c. Choosing the specific study area

The study area is located between 10° latitude north and south of the equator, and 10° longitude east and west of the geostationary subsatellite point. These are the outer limits of a potential study area, however, and not the specific study area for a given case. The study area for each individual case is dependent on the *NOAA-14* orbit trajectory and the location of calibration stripes (e.g., regions of no data) in the HIRS image for that case. HIRS devotes three scan lines to viewing two internal black bodies and space, and there are no earth-sensed radiances available during this calibration procedure. The location of these HIRS calibration stripes differs for each case. In addition, satellite zenith angle considerations preclude the use of the outer edges of the HIRS and AVHRR data. The study area for a given case is chosen entirely using the HIRS image to select an area satisfying the latitude/longitude requirements between the calibration stripes with FOV scan angles less than approximately 14°. Figure 4 shows an example of the study area on a HIRS image.

d. Calculations

The *mean measured radiance* is computed by averaging the spatially smoothed data within the study area for each instrument. A clear-sky radiance is calculated for the location of the FOV with the warmest brightness temperature in the geostationary image near the center of the study area using the forecast model data for estimation of the atmospheric state. Using the FOV with the warmest brightness temperature optimizes the

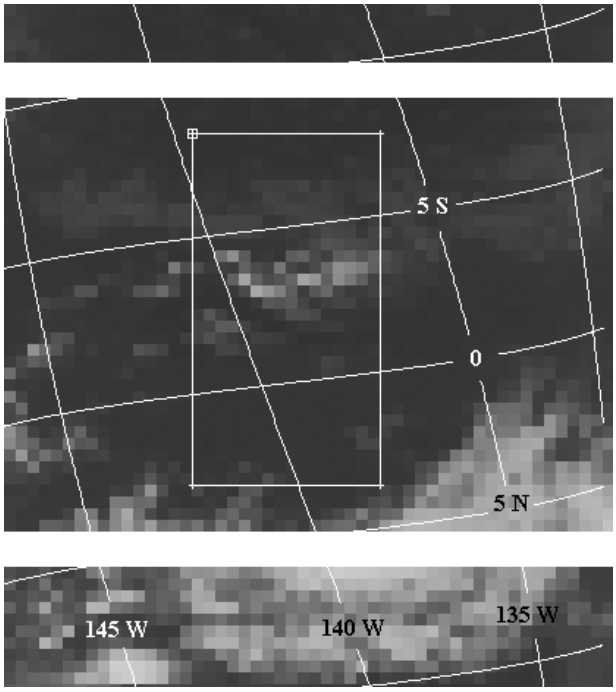

FIG. 4. *NOAA-14* HIRS image from 3 May 2002 (day 123). The study area is depicted by the rectangular region in the center of the image. Note the location of the two white calibration stripes (three lines each).

chances of choosing a cloud-free FOV. The forward model *calculated radiance* is used to account for the differences in the spectral response functions (Figs. 1 and 2). The mean measured radiance difference between geo and leo minus the calculated radiance difference between geo and leo is then attributed to calibration differences between the two instruments. Table 2 shows the mean calibration difference results for the cases covering January 2000 through July 2002. The following paragraphs describe the calculations for a single case in greater detail and section 2e will provide details for a sample case.

The mean radiance in the study area for an individual case is simply the mean of the spatially averaged radiances of all pixels that fall within the study area boundaries (Fig. 5). The calculated radiance is computed using the forward model called Pressure-Layer Fast Algorithm for Atmospheric Transmittances (Hannon et al. 1996) for a 40-level atmospheric profile obtained from the NOGAPS model forecast data (section 2a). The calculated radiance is a best estimate of what the satellite instrument should measure, given the atmospheric state. The difference in the calculated radiances for the two radiometers is used to account for the differences in their spectral response functions.

Thus, in equation form, the radiance intercalibration is given by Eq. (1)

$$\Delta R = [R_{\text{mean}} - R_{\text{calc}}]_{\text{geo}} - [R_{\text{mean}} - R_{\text{calc}}]_{\text{leo}}, \quad (1)$$

where R_{mean} is the mean radiance in the study area, and R_{calc} is the forward model calculated radiance. Conversion to temperatures for a comparison between satellites is accomplished by,

$$\Delta T_{\text{leo}} = [B^{-1}_{\text{mean}} - B^{-1}_{\text{calc}}]_{\text{geo}} - [B^{-1}_{\text{mean}} - B^{-1}_{\text{calc}}]_{\text{leo}}. \quad (2)$$

In Eq. (2) B^{-1} indicates converting radiance to brightness temperature using the inverse Planck function. The HIRS and AVHRR will be substituted for leo in Eq. (2) where appropriate.

There could be a small error associated with the conversion from radiance to brightness temperature if the spectral response function for this calculation is shifted. Spectral response functions for GOES, for example, are expected to be within approximately ± 5 wavenumbers. If the entire spectral response function is shifted ± 5 wavenumbers, the subsequent effect on the brightness temperature is approximately 0.1 K per wavenumber. This holds true for small shifts (less than 5 wavenumbers) in the water vapor channel as well. The standard

TABLE 2. Jan 2000–Jul 2002 (top) IRW and (bottom) WV comparison of geostationary satellites and *NOAA-14* HIRS and AVHRR. The mean, over all cases, measured brightness temperatures for each geostationary satellite are included to provide a crude baseline temperature measurement.

N-14 Delta (geo − leo)		*GOES-8* IRW	*GOES-10* IRW	*Meteosat-5* IRW	*Meteosat-7* IRW	*GMS-5* IRW
No. of comparisons	ΔT_{HIRS}	42	353	352	424	137
	ΔT_{AVHRR}	42	353	352	424	137
Mean	ΔT_{HIRS}	−0.6 K	−0.6 K	−0.8 K	−1.1 K	−0.9 K
	ΔT_{AVHRR}	−0.3 K	−0.1 K	−0.4 K	−0.7 K	−0.6 K
Std dev	ΔT_{HIRS}	0.8 K	1.2 K	1.1 K	1.1 K	1.0 K
	ΔT_{AVHRR}	0.3 K	0.3 K	0.6 K	0.7 K	0.6 K
Mean geo BT		283.2 K	289.1 K	286.0 K	284.7 K	284.4 K
N-14 Delta (geo − leo)		*GOES-8* WV	*GOES-10* WV	*Meteosat-5* WV	*Meteosat-7* WV	*GMS-5* WV
No. of comparisons	ΔT_{HIRS}	237	488	458	327	252
Mean	ΔT_{HIRS}	1.5 K	2.2 K	3.9 K	3.9 K	1.2 K
Std dev	ΔT_{HIRS}	0.7 K	0.8 K	1.3 K	0.8 K	1.0 K
Mean geo BT		244.1 K	247.7 K	244.1 K	247.8 K	244.2 K

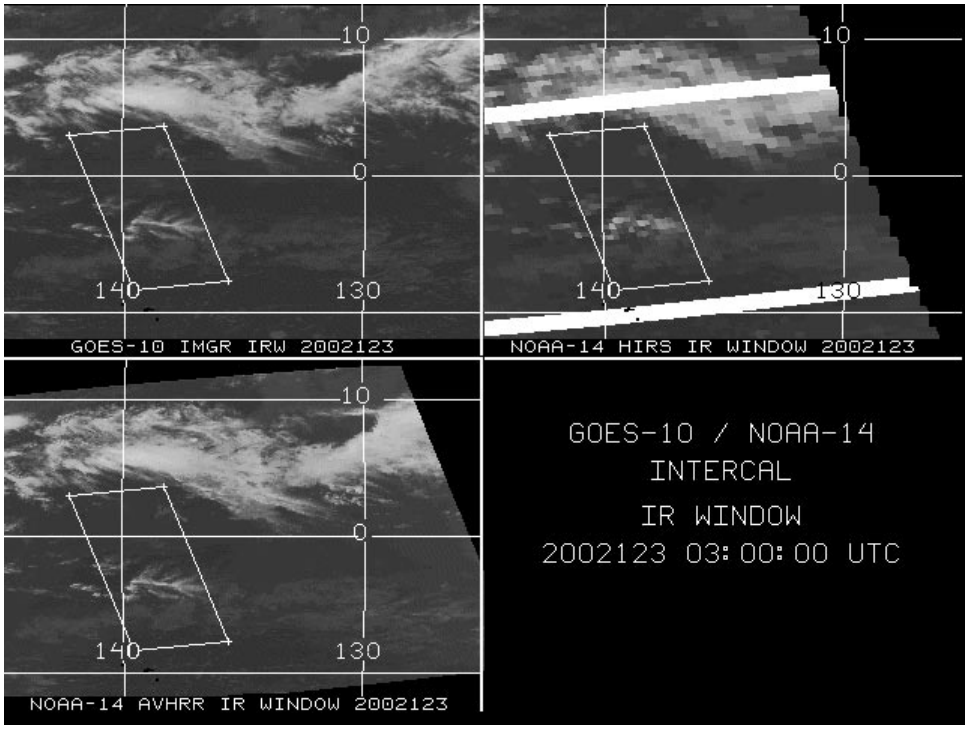

FIG. 5. Example of *GOES-10*, *NOAA-14* HIRS, and *NOAA-14* AVHRR IRW case from 3 May 2002 (day 123). The *NOAA-14* images were remapped into the GOES projection here for display and monitoring purposes only; no remapping of the data is done during processing.

tropical atmosphere was used in Table 3 to demonstrate how the calculated radiances in Eq. (1), converted to brightness temperatures in Eq. (2), can vary between similar bands on different instruments.

e. Sample case details

On 3 May 2002 *NOAA-14* passed over the *GOES-10* subsatellite point (135°W) at approximately 0300 UTC. HIRS, AVHRR, and *GOES-10* infrared window data were collected for that time and location along with NOGAPS atmospheric model data, which was time and space interpolated. The HIRS image was used to determine the study area (Fig. 4), which in this case turned out to be on the order of 600 000 km^2. The scaled radiances for each instrument were then smoothed to an effective 100-km resolution (section 2b). Scaled radiances were converted to radiances, and then the average radiance within the study area is calculated for each instrument. In this example (Fig. 5), the mean radiance (mW m^{-2} cm ster^{-1}) was 97.1 for *GOES-10*, 103.1 for HIRS, and 98.1 for AVHRR. The mean brightness temperature was 291.5 K for *GOES-10*, 291.2 K for HIRS, and 291.3 K for AVHRR. The warmest FOV in the *GOES-10* data was located at 01°15′26″N and 139°16′18″W, which had approximately a 5° satellite zenith angle to each instrument. The vertical profile data from NOGAPS was then interpolated spatially to this location and using that satellite zenith angle, the fast-forward model was used to calculate the clear-sky calculated radiance. The calculated radiance (mW m^{-2} cm ster^{-1}) was 96.0 for *GOES-10*, 100.9 for HIRS, and 96.9 for AVHRR. The associated brightness temperatures were 290.8 K for *GOES-10*, 289.8 K for HIRS, and 290.6 K for AVHRR. Equation (2) was then used to calculate the value for ΔT_{HIRS} (−0.7 K) and ΔT_{AVHRR} (0.0 K). These values are 1 of the 353 values that went into the *GOES-10* IRW column of Table 2.

3. Results

Intercalibration results for all five geostationary satellites covering the time period from January 2000

TABLE 3. Fast-forward model brightness temperature calculated for the standard tropical atmosphere assuming a nadir view in the IRW and WV channels.

Channel	*GOES-8*	*GOES-10*	*Meteosat-5*	*Meteosat-7*	*GMS-5*	HIRS	AVHRR
IRW	295.2	295.3	294.4	294.0	294.3	295.0	295.2
WV	244.3	244.1	243.9	244.2	249.0	244.7	NA

TABLE 4. Jan 2000–Jul 2002 IRW vicarious comparison of geostationary satellites using *NOAA-14* HIRS as a surrogate. Table reads ''column heading minus row heading.''

Using ΔT_{HIRS}	*GOES-8* IRW	*GOES-10* IRW	*Meteosat-5* IRW	*Meteosat-7* IRW	*GMS-5* IRW
GOES-8 IRW		0.0 K	−0.2 K	−0.5 K	−0.3 K
GOES-10 IRW	0.0 K		−0.2 K	−0.5 K	−0.3 K
Meteosat-5 IRW	0.2 K	0.2 K		−0.3 K	−0.1 K
Meteosat-7 IRW	0.5 K	0.5 K	0.3 K		0.2 K
GMS-5 IRW	0.3 K	0.3 K	0.1 K	−0.2 K	

TABLE 5. Jan 2000–Jul 2002 IRW vicarious comparison of geostationary satellites using *NOAA-14* AVHRR as a surrogate. Table reads ''column heading minus row heading.''

Using ΔT_{AVHRR}	*GOES-8* IRW	*GOES-10* IRW	*Meteosat-5* IRW	*Meteosat-7* IRW	*GMS-5* IRW
GOES-8 IRW		0.2 K	−0.1 K	−0.4 K	−0.3 K
GOES-10 IRW	−0.2 K		−0.3 K	−0.6 K	−0.5 K
Meteosat-5 IRW	0.1 K	0.3 K		−0.3 K	−0.2 K
Meteosat-7 IRW	0.4 K	0.6 K	0.3 K		0.1 K
GMS-5 IRW	0.3 K	0.5 K	0.2 K	−0.1 K	

through July 2002 are shown in Table 2. The mean is the average of all cases for the indicated satellite and a negative sign indicates that measurements from the polar-orbiting instrument (HIRS or AVHRR) are warmer than those from the geostationary instrument. All five geostationary instruments on average are measuring colder temperatures than HIRS and AVHRR in the IRW channel; they measure warmer temperatures than HIRS on average in the WV channel. The standard deviation is the deviation about the mean. In the IRW channel the standard deviations for ΔT_{AVHRR} are lower than they are for ΔT_{HIRS}; the standard deviations for the WV channel comparisons are smaller than those in the IRW channel for ΔT_{HIRS}. The results in Table 2 demonstrate that there is good overall agreement between the geo and leo satellites. Vicarious comparisons of results from *GMS-5* and *GOES-8* from a NASA study (Minnis et al. 2002) and Meteosat from a EUMETSAT study (Tjemkes et al. 2001) show reasonably close results given the difference in methods used.

To examine possible seasonal trends the data were divided into the four traditional seasons. Mean temperature differences for each season do not reveal an obvious seasonal dependence. Also there is no evidence of degradation in the measurement results over the course of the study period.

The mean temperature differences in Table 2 may suggest comparisons between HIRS and the geostationary satellites are made difficult by the relatively narrow HIRS spectral response function (Fig. 1) and large FOV size compared to the other instruments. IRW results between AVHRR and all five geostationary instruments show smaller differences. For all geostationary instruments, comparison to HIRS is more favorable in the IRW channel than in the WV channel. This suggests a higher degree of difficulty to compare different instruments in the WV channel. This is possibly due to the widely different spectral response functions (Fig. 2), a higher degree of uncertainty in the WV calibration as the WV scene temperature is roughly 40 K colder than the onboard blackbody references, and the greater inhomogeneity of the atmospheric water vapor structure.

4. Conclusions

The mean differences of all five geostationary instruments appear to be calibrated to within approximately 0.5 K of each other in the infrared window channel. It is not possible, from this study, to determine which geostationary or polar-orbiting satellite is the most accurate or has the best absolute calibration. Tables 4 and 5 show how the geostationary instruments compare in the IRW band using *NOAA-14* HIRS and AVHRR as a surrogate. Comparisons in the WV band using *NOAA-14* HIRS show more variability (Table 6); they compare to within 2.7 K. *GOES-8*, *-10*, and *GMS-5* form one group that compare favorably to each other and *Meteosat-5* and *-7* form another. *Meteosat-7* is used to calibrate *Meteosat-5* so a favorable comparison is expected and reflects a successful use of vicarious calibration methods.

The mean temperature differences in the IRW channels are small compared to those in the WV channels, but the standard deviations generally follow the opposite trend when using HIRS. Standard deviations in the IRW channel may be larger due to the greater variability in IRW radiances as compared to radiances in the WV channel. The IRW channel will measure surface effects as well as clouds and the range of radiances (and brightness temperatures) will be much greater than that of the

TABLE 6. Jan 2000–Jul 2002 WV vicarious comparison of geostationary satellites using *NOAA-14* HIRS as a surrogate. Table reads ''column heading minus row heading.''

Using ΔT_{HIRS}	*GOES-8* WV	*GOES-10* WV	*Meteosat-5* WV	*Meteosat-7* WV	*GMS-5* WV
GOES-8 WV		0.7 K	2.4 K	2.4 K	−0.3 K
GOES-10 WV	−0.7 K		1.7 K	1.7 K	−1.0 K
Meteosat-5 WV	−2.4 K	−1.7 K		0.0 K	−2.7 K
Meteosat-7 WV	−2.4 K	−1.7 K	0.0 K		−2.7 K
GMS-5 WV	0.3 K	1.0 K	2.7 K	2.7 K	

water vapor channel, which only measures a small range of radiances (and brightness temperatures) from higher in the atmospheric column.

In general, these satellite intercalibration results should be viewed as reassuring for those doing global studies involving more than one instrument. The satellites are all within an acceptable range of differences in the infrared window channel. The water vapor channel results are less assuring; yet this may point to the need for a better understanding of the atmospheric state in the water absorption region of the earth-emitted spectra.

5. Future work

Work has begun to apply the same methods to other instruments. HIRS and AVHRR on *NOAA-15* and *NOAA-16* will become a part of the routine processing. *GOES-12*, with a spectrally wider water vapor channel, will also be included (Schmit et al. 2001). With NASA's *Aqua* launched in May 2002 there is a Moderate Resolution Imaging Spectroradiometer (MODIS) as well as the high spectral resolution Advanced Infrared Sounder (AIRS) available. MODIS calibration should be more stable than that of *NOAA-14* AVHRR or HIRS (Guenther et al. 1996). AIRS, and ultimately the operational Crosstrack Infrared Sounder, will allow for more detailed comparison of radiances from one leo to multiple geo satellites. Comparisons with a more accurately calibrated polar-orbiting, high spectral resolution instrument will provide more insight as to how well the geostationary instruments are spectrally characterized. Preliminary results in a *GOES-10* comparison to AIRS showed extremely well matched average scene temperatures within 0.2 K for the infrared window channel. In the near future Meteosat Second Generation data will be available with expected improvements in calibration over the previous generation of Meteosat instruments, including the use of radiance units consistent with those on the other operational geostationary instruments (Schmetz et al. 2002).

Acknowledgments. The authors would like to thank James P. Nelson III, Hal Woolf, and Geary Callan for their programming assistance. This research was performed primarily under NOAA Grant NA07EC0676.

REFERENCES

Counet, P. A., Ed., 2001: *Report of the 29th Meeting of the Coordination Group for Meteorological Satellites.* EUMETSAT, CD-ROM.

Desormeaux, Y., W. B. Rossow, C. L. Brest, and G. G. Campbel, 1993: Normalization and calibration of geostationary satellite radiances for the International Satellite Cloud Climatology Project. *J. Amos. Oceanic Technol.,* **10,** 304–325.

Ellrod, G. P., 1996: The use of *GOES-8* multispectral imagery for the detection of aircraft icing regions. Preprints, *Eighth Conf. on Satellite Meteorology and Oceanography,* Atlanta, GA, Amer. Meteor. Soc., 168–171.

EUMETSAT, 2000: The Meteosat system. EUM Tech. Doc. 05, Revision 4, 66 pp.

Guenther, B., and Coauthors, 1996: MODIS calibration: A brief review of the strategy for the at-launch calibration approach. *J. Atmos. Oceanic Technol.,* **13,** 274–285.

Gunshor, M. M., T. J. Schmit, and W. P. Menzel, 2001: Intercalibration of geostationary and polar-orbiting infrared window and water vapor radiances. *Extended Abstracts, 11th Conf. on Satellite Meteorology and Oceanography,* Madison, WI, Amer. Meteor. Soc., 438–441.

Hannon, S., L. L. Strow, and W. W. McMillan, 1996: Atmospheric infrared fast transmittance models: A comparison of two approaches. *Proc. Optical Spectroscopic Techniques and Instrumentation for Atmospheric and Space Research,* Denver, CO, Inter. Soc. for Opt. Eng., 94–105.

Kidwell, K. B., Ed., 1998: NOAA Polar Orbiter Data User's Guide. NOAA. [Available online at www2.ncdc.noaa.gov/docs/podug/.]

Menzel, W. P., and J. F. W. Purdom, 1994: Introducing *GOES-I*: The first of a new generation of geostationary operational environmental satellites. *Bull. Amer. Meteor. Soc.,* **75,** 757–781.

——, W. L. Smith, and L. D. Herman, 1981: Visible infrared spin-can radiometer atmospheric sounder radiometric calibration: An inflight evaluation from intercomparison with HIRS and radiosonde measurements. *Appl. Opt.,* **20,** 3641–3644.

——, J. Schmetz, S. Nieman, L. van de Berg, V. Gaertner, and T. J. Schmit, 1993: Intercomparison of the operational calibration of *GOES-7* and *Meteosat-3/4.* NOAA Tech. Rep. NESDIS 73, 14 pp.

——, F. C. Holt, T. J. Schmit, R. M. Aune, G. S. Wade, D. G. Gray, and A. J. Schreiner, 1998: Application of *GOES-8/9* soundings to weather forecasting and nowcasting. *Bull. Amer. Meteor. Soc.,* **79,** 2059–2078.

Minnis, P., L. Nguyen, D. R. Doelling, D. F. Young, W. F. Miller, and D. P. Kratz, 2002: Rapid calibration of operational and research meteorological satellite imagers. Part II: Comparison of infrared channels. *J. Atmos. Oceanic Technol.,* **19,** 1250–1266.

NASA, 1996: *GOES I-M DataBook.* Revision 1, 186 pp.

Rosmond, T. E., 1992: The design and testing of the Navy Operational Global Atmospheric Prediction System. *Wea. Forecasting,* **7,** 262–272.

Schmetz, J., P. Pili, S. Tjemkes, D. Just, J. Kerkmann, S. Rota, and A. Ratier, 2002: An Introduction to Meteosat Second Generation (MSG). *Bull. Amer. Meteor. Soc.,* **83,** 977–992.

Schmit, T. J., and L. D. Herman, 1992: Comparison of multi-spectral data: *GOES-7* (VAS) to *NOAA-11* (HIRS). Preprints, *Sixth Conf. on Satellite Meteorology and Oceanography,* Atlanta, GA, Amer. Meteor. Soc., 258–259.

——, E. M. Prins, A. J. Schreiner, and J. J. Gurka, 2001: Introducing the *GOES-M* Imager. *Natl. Wea. Assoc. Digest,* **25,** 28–37.

Suziki, T., 1997: *The GMS User's Guide.* 3d ed. Meteorological Satellite Center Tokyo, 190 pp.

Tjemkes, S. A., M. Koenig, H.-J. Lutz, L. van de Berg, and J. Schmetz, 2001: Calibration of Meteosat water vapor channel observations with independent satellite observations. *J. Geophys. Res.,* **106,** 5199–5209.

Wanzong, S., W. P. Menzel, and G. Callan, 1998: Intercalibration of GOES, Meteosat, GMS, HIRS, and AVHRR infrared radiances. Preprints, *Ninth Conf. on Satellite Meteorology and Oceanography,* Paris, France, Amer. Meteor. Soc., 714–717.

Weinreb, M. P., M. Jamison, N. Fulton, Y. Chen, J. X. Johnson, J. Bremer, C. Smith, and J. Baucom, 1997: Operational calibration of *Geostationary Operational Environmental Satellite-8* and *-9* imagers and sounders. *Appl. Opt.,* **36,** 6895–6904.

Wu, X., W. P. Menzel, and G. S. Wade, 1999: Estimation of sea surface temperatures using *GOES-8/9* radiance measurements. *Bull. Amer. Meteor. Soc.,* **80,** 1127–1138.